

Docmarking: Real-Time Screen-Cam Robust Document Image Watermarking

Aleksey Yakushev*, Yury Markin*, Dmitry Obydenkov*, Alexander Frolov*, Stas Fomin*,
Manuk Akopyan*, Alexander Kozachok[†] and Arthur Gaynov[‡]

*Ivannikov Institute for System Programming of the RAS

{yakushev, uistas, obydenkov, aefrolov, fomin, manuk}@ispras.ru

Moscow, Russia

[†]Russian Federation Security Guard Service Federal Academy

a.kozachok@academ.msk.rsnet.ru

Oryol, Russia

[‡]Ministry of Defence of the Russian Federation

gae@mil.ru

Moscow, Russia

Abstract—This paper focuses on investigation of confidential documents leaks in the form of screen photographs. Proposed approach does not try to prevent leak in the first place but rather aims to determine source of the leak. Method works by applying on the screen a unique identifying watermark as semi-transparent image that is almost imperceptible for human eyes. Watermark image is static and stays on the screen all the time thus watermark present on every captured photograph of the screen. The key components of the approach are three neural networks. The first network generates an image with embedded message in a way that this image is almost invisible when displayed on the screen. The other two neural networks are used to retrieve embedded message with high accuracy. Developed method was comprehensively tested on different screen and cameras. Test results showed high efficiency of the proposed approach.

Index Terms—document leakage investigation, screen-cam robust watermarking, blind watermarking

I. INTRODUCTION

With the growth of computing power and the acceleration of data processing, more and more areas of human activity are transferred to the digital space. In particular, usage of electronic documents is growing. Many organizations that use electronic documents in their processes face document leakage problem. Leaked documents may contain confidential information intended only for certain company employees. Their transfer to third parties may cause serious financial and reputational losses.

According to the InfoWatch analytical center report on the study of restricted information leaks in Russia in 2020 [1], 79% of leaks were provoked by insiders, and 79.3% of them were committed intentionally. To prevent insider leaks, Data Leakage Prevention (DLP) systems are implemented. DLP solutions are software and hardware systems that prohibit (active DLP) or register (passive DLP) the actions of company employees when they are working with certain software. These actions include: sending confidential files via email, using removable USB drives, sending files to cloud storage, etc.

Yakushev A., Markin Yu., Obydenkov D., Frolov A., Fomin S., Akopyan M., Kozachok A., Gaynov A. Docmarking: Real-Time Screen-Cam Robust Document Image Watermarking. 2022 Ivannikov Ispras Open Conference (ISPRAS). IEEE, 2022, pp. 142-150, DOI: 10.1109/ISPRAS57371.2022.10076265.
© 2022 IEEE. Personal use of this material is permitted. Permission from IEEE must be obtained for all other uses, in any current or future media, including reprinting/republishing this material for advertising or promotional purposes, creating new collective works, for resale or redistribution to servers or lists, or reuse of any copyrighted component of this work in other works.

However, DLP systems do not cover all leak channels, namely, printed copies and photographs of confidential documents displayed on workstation monitor. Printed copies may be physically moved out from protected perimeter and scans or photographs of printed documents may be anonymously published or send to outsiders (*print-cam* and *print-scan* scenarios). Screen photographs can be easily taken, as nowadays everyone has personal smartphone with high quality camera, which may be used to breach sensitive information from the screen (*screen-cam* scenario).

This study propose data leakage investigations approach committed by insiders using personal smartphone cameras and workstations. It is supposed that employee intentionally or occasionally may take a photograph of a monitor with confidential information displayed. Organization provides workstation with preinstalled software, which imposes imperceptible watermark on whole monitor area. Each employee is associated with a unique watermark that allows to identify the department, user, device, and time of activity. If the employee takes a photograph of the screen with sensitive information, the photograph contains watermark. The spreading of watermarked photographs is undesirable. After getting the photograph the organization security officer can conduct investigation, extract the watermark, and determine the cause of the leakage. Since the investigation is conducted *post factum*, human guided processing of the watermarked image and slow decoding algorithms can be applied. The described problem has become a basis for the development of screen watermarking software solution.

II. RELATED WORKS

A. Watermarking Methods Typology

Early studies in data watermarking were published in '90s, basic ideas were developed further and dozens of articles appeared during this period [2]–[4]. Researchers classify watermarking techniques by the type of content: text, image, video or audio data. Usually watermarking algorithm focuses

on specific type of data and works inefficiently on other types. Text documents watermarking approaches may be divided into frequency or spatial domain. Discrete Fourier Transform (DFT) [5] and Discrete Cosine Transform (DCT) [6] based methods refer to the frequency domain. The spatial domain methods apply document modification using information about document text structure: layout, semantic or syntax language properties, format features, etc. They are subdivided into structural and linguistic methods [7].

B. Methods for Watermarking Document Images on the Screen

The authors of the paper [8] proposed a method for marking text documents based on a smooth change in the brightness of screen image areas. The watermark is embedded by lowering or brightening the circular areas, depending on the value of the watermark message bits. A smooth change in brightness is imperceptible to human eyes, but is distinguishable by a digital camera. Fig. 1a is an example of a screen photograph with a marked image. Authors tested the method on edited (scaling, color correction, brightness, contrast, white balance) and unedited screen photographs. However, the impact of shooting angle and image compression on the extraction accuracy was not studied.

The second approach [9], developed as a part of the document watermarking system [10], is also based on smooth brightness changes on the screen. The watermark is embedded by placing a sequence of rectangular areas of various brightness into text line spacing. Imperceptibility of the watermark is based on the assumption that changes in brightness are less visible between the text lines than on wide plain areas (margins). Fig. 1b is an example of a marked document. To embed the watermark, algorithm performs document line spacing search on the screen image. Delay for rendering the watermark image reaches a few hundreds milliseconds, so the approach causes visual discomfort for users due to insufficient UI responsiveness.

Under the other approach watermarking of documents images displayed on the screen is implemented by using neural network [11]. The watermark on document image is rather imperceptible (Fig. 1c); the extraction neural network provides high accuracy. The authors of the article compared the proposed method with common images watermarking methods robust to screen-cam process. The comparison showed a significant advantage of the new approach in document image watermarking. Watermarking of all documents in real time mode on the screen requires frequent launch of embedding neural network which may need high processing speed. It seems that practical usage of the approach may cause significant difficulties.

In the work [12] the watermark is embedded as a visible noisy template on text background, referred to as underground. The watermark is designed not to be imperceptible, but inconspicuous, that means it doesn't affect readability of the text and that it can't be extracted without specific algorithm. As the watermark is visible, the approach doesn't meet the requirement of watermark imperceptibility.

leave you. I must find mode: Для предотвращения и/или рас zation index modulation (QIM), :
of her conference with her o ции используются технологии which can be a stream cipher alg
: who should omit an morni o основанные на DLP технологии cipher algorithm (e.g., AES). Our
ent was admitted at looking o комплексы, ведущие мониторы embedded security attributes in t
n, who, from our manner of p образом реагирующие на эти д : rest of this paper is organized as
ppiness! But it was not to be : доступ к сети Интернет, запр : dependently present the waterm
off as fast as I certainly lool : записывать действия сотрудни : times we used, before introducin
from [12]) : ющие DLP системы не позво : n III. We then detail our implem
photographing экрана мон : n V presents some experimental
фиденциального документа. Д : t medical modalities, ultrasound

a) Example of [8] b) Example of [9] c) Example of [11]
marking (taken marking marking
from [12])

Fig. 1. Examples of images marked with existing screen-cam robust methods.

In [13] quite similar to [8] idea of brightness symbols is used, but imperceptibility is reached in a different way. If the refresh rate of screen image is high enough, two subsequent frames displayed on the screen may superimpose for human perception, but still can be distinguished by digital camera. Two subsequent frames contain opposite watermark images, so that their superposition looks like not marked image. Nevertheless, digital camera captures one of the two frames, so that the photograph of the screen contains watermark. The drawback of this approach is that it may show low visual quality on most common monitors with the refresh rate of 60 Hz or less.

The usage of moiré pattern for watermark embedding is proposed in [14] (see III-A for more information about moiré pattern). Special template is drawn on screen image, that causes moiré pattern appearance on the captured screen photograph. The template specifies the form of the moiré pattern, allowing to embed multibit watermark and pass it to camera via moiré effect. The method has a serious disadvantage: it works only under restricted shooting conditions including low range of distances and angles between camera and screen. Also it has rather low embedding capacity of 14 bits.

All reviewed studies have serious drawbacks, that may face difficulties with implementation of a software solution that fit the previously mentioned problem statement.

III. PROPOSED APPROACH

A. Watermark Screen-Shooting Robustness

Embedded watermark must be decoded as accurate as possible, but remain as imperceptible as possible. Likewise watermarking algorithm must be robust to different image distortions caused by conversion from digital to analog domain and vice versa, lossy compression, and other factors. This leads to the need to consider in detail the nature of distortions that can be divided into groups, depending on the moment of their appearance.

The first group of distortions is directly related to the process of displaying an image on the screen. In this case, the digital signal is converted to analog. Different monitors significantly vary in their ability to convert the numerical pixel values of an image into the color and luminosity captured by the human eye or a digital camera. The image is also affected by the characteristics and settings of the monitor.

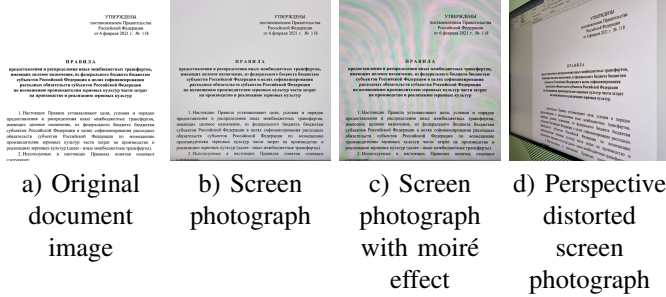


Fig. 2. Photographs of screen displaying document.

Distortions from the second group occur at the moment of screen photographing and depend on the photographing conditions. The camera may be located at different distance and angle from the screen, so the original shape and scale of the image may change. By the way light is passing thought camera optical system causing different optical effects such as barrel distortion. Shooting conditions are also affected by the presence of additional light sources and camera focus.

It is important to mention distortion that occurs when photographing a screen — the moiré effect. Usually, the moiré effect on screen photographs looks like a set of bands of different colors with a non-periodic structure. The thickness of these bands is not constant and varies in different parts of the photograph. The moiré effect occurs when two periodic structures located with some deviation relative to each other are superimposed. So, when photographing the screen, the pixels of the screen matrix and the sensors of the camera matrix act as such structures. At the moment, the problem of removing the moiré effect from photographs to improve their quality is actively studied [15], including screen photographs [16].

The third group of distortions refers to a set of algorithms for processing the resulting photograph on the camera device. Conversion from analog signal domain to digital image significantly differs. Camera matrices have different light sensitivity, camera manufacturers use various raw photograph enhance algorithms. And finally, photo is saved into file using lossy compression algorithm. To sum up, screen cam scenario specific distortions consider serious efforts to achieve acceptable robustness and should be considered while testing.

B. Overview of the Proposed Watermarking Method

The scheme of developed screen watermarking method is shown in Fig. 3. The encoder neural network E takes a message $m, m_i \in \{0, 1\}, i \in \{1, \dots, M\}$ as input (the method was tested with $M = 50$) and generates a greyscale watermark image I_w with a fixed size $S \times S \times 1$ ($S = 120$ in the implementation). The main properties of image I_w are as follows:

- The image I_w consists of smooth brightness transitions;
- Smooth brightness transitions are preserved if two identical I_w images are combined, placed either side by side or one above the other.

An image I_o is formed by composing several images I_w placed side by side in the form of a grid. So, for a screen with a

resolution of 1920×1080 and $S = 120$, a grid is composed of 16×9 images I_w .

The generated image I_o is displayed on the screen with some opacity and covers the screen image I_s . It creates smooth transitions of brightness on the displayed image I'_s due to the described property.

As the encoder network does not use the current screen image I_s to create watermark image, I_o remains static no matter what the user of the device does. Cover image I_o can be generated once and used through the whole work flow. Also, static image I_o does not cause discomfort when working with the device. The watermark always present on the screen, which allows the method to be used in real-time.

The watermark m' is extracted from the photograph of the screen, with perspective correction and cropping of non-screen areas beforehand. Due to the periodic structure of the image I_o , the watermark presents in all areas of the screen and can be extracted from a photograph of any sufficiently large part of it. The periodicity of the I_o image is used by watermark extraction algorithm. Firstly the algorithm determines the value of the period p in the photograph. Then, an image I''_w is calculated as the average brightness of $p \times p$ areas of the photograph with a p step. As the top left point of photograph not necessary coincide top left point of screen, the image I''_w may be cyclically shifted relative to I_w . Using the neural network D_c , the value of this shift is determined. The image I'_w is obtained by cyclically shifting the image I''_w by the opposite value. Then the decoder network D_w is used to determine the bit values of the extracted watermark m' .

C. Architecture of the Neural Networks

The encoder neural network E is used to create an image of a watermark I_w of size $S \times S \times 1$ from a message bit sequence of m . It consists of 2 parts. Firstly an M bit sequence is passed to a fully connected layer in order to obtain a tensor consisting of S^2 elements. The resulting tensor is reshaped to the $S \times S \times 1$ format. It can be interpreted as some preliminary image. Secondly the tensor is passed to the main part of the encoder network E with close to U-Net [17] architecture.

An important difference between neural network E and the classic U-Net architecture is the usage of circular padding. It determines the behavior of convolutional layers on the tensor borders. The tensor border is processed as if there is a copy of this tensor in the continuation of this border. Circular padding is used, for example, in the problem of 360° photographs processing [18]. The neural network that receives such images shall take into account that the areas on the left and right borders of the photograph smoothly transit into each other, and this is accomplished by applying circular padding along the horizontal axis. In the encoder network E this technique is used both along the horizontal and vertical axes. The main goal of circular padding usage is to make brightness transition on the image I_o as smooth as possible.

In the process of watermark extraction, the image I''_w may be cyclically shifted relative to the image I_w . The neural network D_c is used to find the value of the cyclic shift. The input of

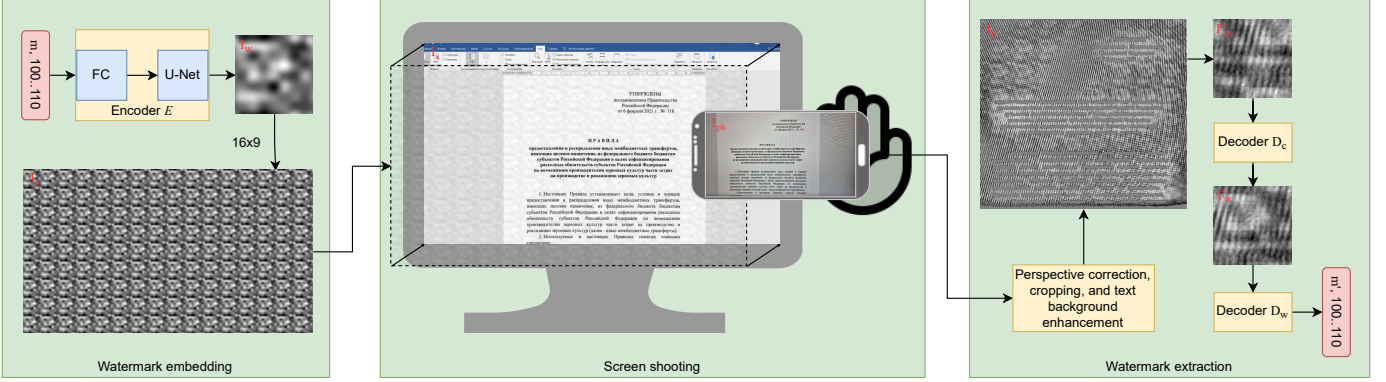


Fig. 3. Scheme of the proposed method.

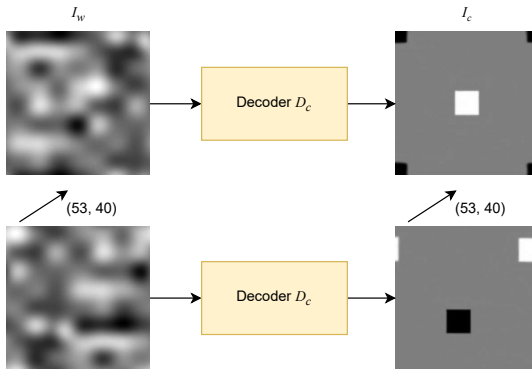


Fig. 4. Decoder D_c invariance to the cyclic shift of the input image.

the network D_c is the $S \times S \times 1$ image I''_w . The network D_c has the same U-Net architecture as the second part of the neural network E , including circular padding. If the input D_c is the watermark image I_w , the tensor I_c of size $S \times S \times 1$ is obtained, filled with the following values:

$$I_c(x, y) = \begin{cases} 1, & \frac{S}{2} - c \leq x, y \leq \frac{S}{2} + c \\ -1, & (0 \leq x \leq c \text{ or } S - c \leq x \leq S) \text{ and} \\ & (0 \leq y \leq c \text{ or } S - c \leq y \leq S) \\ 0, & \text{otherwise} \end{cases} \quad (1)$$

where c — some given size of center area.

The main property of D_c is the invariance to the cyclic shift of the input image (Fig. 4). So, if D_c is applied to the image I_w , cyclically shifted by some values $(\Delta x, \Delta y)$, the output will be I_c tensor shifted by the same values. The shift values can be determined by searching for the position of the maximum of the output tensor relative to its center. In the process of watermark extraction, D_c is used to determine value of the cyclic shift of the image I''_w in order to obtain the image I'_w , which differs from I_w by noise caused by the screen shooting process.

The problem of extracting the watermark w' from the image I'_w can be interpreted as a multilabel image classification problem. Thus, if the bit of the watermark w_i is equal to 1, it means

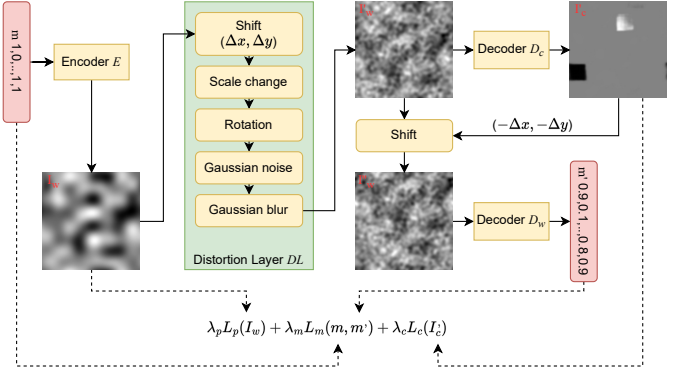


Fig. 5. Neural networks training scheme.

that image belongs to the class with label i . Neural network architectures specialized on classification problems can be used as extraction neural network D_w . In the implementation of the proposed method, the EfficientNet-B2 [19] architecture has been chosen. The EfficientNet architecture class was obtained using the NAS (Neural Architecture Search) method. With the same number of trainable parameters, EfficientNet neural networks show the highest accuracy compared to other neural network architectures in the ImageNet [20] classification problem.

D. Neural Networks Training

The neural networks E , D_c and D_w are trained simultaneously (Fig. 5). Each training iteration consists of the following steps. First, a random sequence of M bits is generated that defines message m . Based on the message m , the neural network E creates an image of the watermark I_w . The image I_w is transformed by the distorting layer DL . The resulting image I''_w is passed to the neural network D_c returning the tensor I'_c . The value of the cyclic shift $(\Delta x, \Delta y)$ of the image I''_w is determined from the position of the I'_c tensor maximum. The image I'_w is formed by a reverse shift by $(-\Delta x, -\Delta y)$ of the image I''_w . The neural network D_w takes the image I'_w to obtain the extracted M bit sequence m' . Then the loss function

L is calculated. The loss function gradient is used to update the parameters of the neural networks E , D_c and D_w .

The distortion layer DL is used to make changes to the image I_w . Its main task is to simulate the transformations that occur when photographing the screen during neural networks training. DL consists of the following steps, performed sequentially:

- 1) Random shift by $(\Delta x, \Delta y)$;
- 2) Random scale change within $(0.96; 1.04)$;
- 3) Rotation by a random angle within $(-2^\circ; 2^\circ)$;
- 4) Applying Gaussian noise $\mathcal{N}(0, 1)$;
- 5) Applying Gaussian blur with variance 1.

The loss function L used in the learning process consists of three parts:

$$L = \lambda_p L_p + \lambda_c L_c + \lambda_m L_m, \quad (2)$$

where λ_p , λ_c , λ_m are the weights of loss functions.

Function L_p specifies the property of a smooth brightness transition on the image I_w . Each pixel of image I_w is compared with its neighbors in a window of size 3×3 :

$$L_p = \sqrt{\frac{1}{9S^2} \sum_{\substack{x=1..S \\ y=1..S \\ \delta x \in \{-1, 0, 1\} \\ \delta y \in \{-1, 0, 1\}}} (I_w(x, y) - I_w(x + \delta x, y + \delta y))^2}, \quad (3)$$

with circular transition on borders:

$$\begin{aligned} x \notin \{1, \dots, S\} \Rightarrow x &:= ((x - 1) \bmod S) + 1, \\ y \notin \{1, \dots, S\} \Rightarrow y &:= ((y - 1) \bmod S) + 1. \end{aligned} \quad (4)$$

Due to the conditions 4, the smooth brightness transition on the image I_w has the property of cyclicity.

The function L_c is used to train neural network D_c to determine shift value $(\Delta x, \Delta y)$. To do this, the I_c tensor is cyclically shifted by $(\Delta x, \Delta y)$, taking into account conditions 4:

$$I_c^{shifted}(x, y) = I_c(x - \Delta x, y - \Delta y). \quad (5)$$

The I'_c tensor is compared with the resulting $I_c^{shifted}$ tensor:

$$L_c = \sqrt{\frac{1}{S^2} \sum_{x=1..S} (I'_c(x, y) - I_c^{shifted}(x, y))^2}. \quad (6)$$

The function L_w is responsible for the accuracy of the extracted message. As mentioned, the task of watermark extracting from an image is similar to an image classification problem, so the binary cross-entropy function can be used to compare the bits of the embedded message m and the extracted message m' :

$$L_w = -\frac{1}{M} \sum_{i=1}^M m_i \log m'_i + (1 - m_i) \log (1 - m'_i). \quad (7)$$

E. Embedding the Watermark Image on the Screen

To generate and embed watermark image special software is used. It is installed on the employee device of the organization that uses the proposed method to protect text documents on the screen. The watermarking software interacts with the graphic subsystem of the operating system of the employee's device. It displays the I_o image containing the watermark in a window, permanently located on the top of all windows in operating system. The window is fully transparent to user input (keyboard and mouse clicks) and semi-transparent visually with opacity parameter $\alpha \in [0, 1]$. According to the rules for adding partially transparent images [21], the pixel values of the image I'_s displayed on the screen are calculated as follows:

$$I'_s(x, y) = (1 - \alpha) \cdot I_s^c(x, y) + \alpha \cdot I_o(x, y), \quad (8)$$

where $c \in \{R, G, B\}$ denotes the red, green, and blue color channels. The opacity parameter α determines the imperceptibility of the watermark on the screen. Examples of marked images with different values of α are shown in Fig. 6.

F. Watermark Extraction Algorithm

A photograph of a document on a screen that has become publicly available is used by an organization's security analyst to investigate a leak. Only the leaked photograph is required for the investigation that makes the proposed approach blind. It is assumed that the investigation may take some time, thus watermark extraction algorithm does not have to be very fast. Moreover, the watermark extraction can be performed repeatedly — with different algorithm parameters, and some extraction steps can be performed by the analyst using third-party image processing software. The watermark extraction is conducted in several steps:

- 1) Perspective correction and cropping of non-screen parts of the photograph (done by the analyst beforehand);
- 2) Detection of background areas in the document photograph, getting image I_b ;
- 3) Searching for a periodic structure in the image I_b , determining the period p ;
- 4) Averaging I_b with step p up to $p \times p$ image I_p , rescaling it to obtain the image I''_w of size $S \times S$;
- 5) Cyclic shift of the image I''_w using the neural network D_c resulting in the image I'_w ;
- 6) Extracting the bit values of the message m' from the image I'_w by applying the neural network D_w .

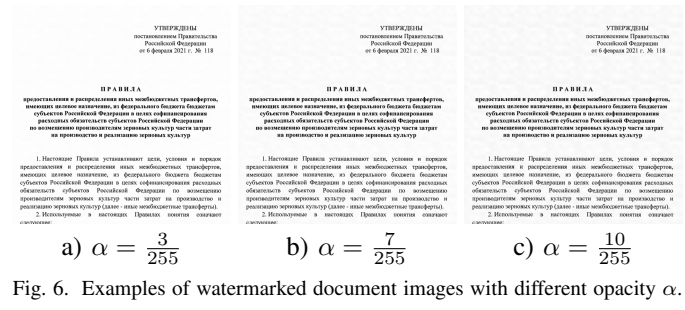


Fig. 6. Examples of watermarked document images with different opacity α .

In most cases, screen photographs are made at some angle to the screen. Thus, screen image perspective on the photograph is distorted. The first step in the watermark extraction is to correct the perspective of the photograph. It can be performed by an analyst using image editing software. The corrected photograph is cropped in order to leave only the areas related to the screen in the final image.

The cropped photograph is converted to grayscale denoted as I_{ph} . To determine the background areas in the document in the image I_{ph} (step 2), the value in each pixel is compared to the median value in a window of the given size $a \times a$ centered on that pixel.

Image I_b is calculated as follows:

$$I_b(x, y) = \begin{cases} I_{ph}(x, y) - I_{ph}^a(x, y), & |I_{ph}(x, y) - I_{ph}^a(x, y)| \leq t, \\ 0, & |I_{ph}(x, y) - I_{ph}^a(x, y)| > t, \end{cases} \quad (9)$$

where $I_{ph}^a(x, y)$ is the median value of I_{ph} in a window of size $a \times a$ centered at (x, y) ; t is specified threshold value.

Image of a text document is a set of mostly black characters on plain, often white, background. Due to this property, displayed image I'_s is close to I_o in the document background areas. As I_o is a grid of I_w images, it has a periodic structure with period S . Periodic structure is preserved on photograph document background but it has different period p due to scaling. The purpose of the third step watermark extraction step is to determine the value of the period p in the image I_b . Denote by I_p the averaging of the image I_b with the step p :

$$I_p(x, y) = \frac{1}{\lfloor \frac{W}{p} \rfloor \cdot \lfloor \frac{H}{p} \rfloor} \sum_{k, l=1}^{\lfloor \frac{W}{p} \rfloor, \lfloor \frac{H}{p} \rfloor} I_b(k \cdot p + x, l \cdot p + y). \quad (10)$$

Period determination is based on the following observation. If the p value does not correspond to the desired period, the distribution of the image I_p pixel values turns out to be close to random noise. After removing the noise using the Gaussian filter $G(\cdot)$, the image becomes very monotone. The standard deviation $std(\cdot)$ of this image is close to 0. Alternatively, If p coincides with the period, applying the Gaussian filter to I_p preserves the brightness transitions and the standard deviation is higher than zero. Thus, the period can be determined by searching the maximum of the following:

$$p = \arg \max_{p' \in [p_0, \dots, p_1]} std(G(I_{p'})). \quad (11)$$

The averaging of the image I_b at the fourth step also conducted according to the Eq. 10. The image I_p obtained by averaging I_b is rescaled from $p \times p$ to $S \times S$, resulting in the image I''_w . The further watermark extraction steps are the same as in processing of the image I''_w during neural networks training described in the III-D section.

IV. EXPERIMENTAL RESULTS AND ANALYSIS

Proposed watermarking method was implemented with watermark capacity $M = 50$ bits and watermark image I_w with size $S = 120$. Neural networks E , D_c and D_w were

trained with the Adam optimizer [22]. In total, 1440000 50-bit sequences were generated during the training process.

In the practical application of the proposed watermarking method a 32-bit message is embedded. 18 bits of BCH error correction codes [23] are added to the message, allowing to correct up to 3 errors in the received 50-bit sequence. Thus, we can assume that the watermark is extracted correctly if there are no more than 3 errors.

To test the method photographs of monitor screens with displayed images of documents were taken. The websites of the Ministry of Education and Science of the Russian Federation [24] and the Ministry of Finance of the Russian Federation [25] were chosen as sources for the document images. The experiments involved 3 monitors and 3 smartphones. Monitor characteristics are given in the Table I, and the smartphone digital cameras characteristics are given in the Table II. The experiments were carried out using the default camera application on each smartphone in automatic mode.

A. Selecting the Opacity of the Marking Window

As mentioned in section III-E, the imperceptibility of the watermark on the screen is affected by the value of marking window opacity α . Based on the implementation features, it is convenient to represent the values of α in fractions of the form $n/255$, where n is an integer. To determine the degree of imperceptibility, the Peak Signal to Noise Ratio (PSNR) and Structural Similarity Metric (SSIM) [26] were chosen as imperceptibility metrics. Metrics were averaged over images of 50 marked documents. Since it is assumed that the watermark is displayed regardless of the screen image, it is important to make it imperceptible not only on document images, but also on common images. Imperceptibility metrics were also calculated for 50 common images taken from the Open Images V6 dataset [27]. The results of imperceptibility metrics calculating for different values of α are presented in the Table III.

Increasing the opacity α of marking window leads to an increase in the visibility of the watermark. According to the SSIM metric, the method demonstrates high imperceptibility for all α values used in testing. The PSNR metric shows that the embedded watermark is less visible on common images than on document images. For values of α not exceeding 5/255, the watermark is hardly noticeable.

TABLE I
MONITOR CHARACTERISTICS

Monitor	Matrix Type	Screen Resolution	Refresh Rate
Samsung SM 940FN	TFT PVA	1280 × 1024	75Hz
Sony SDM-S75A	TN	1280 × 1024	75Hz
Dell U2722D	IPS	2560 × 1440	60Hz

TABLE II
CAMERA CHARACTERISTICS

Smartphone	Resolution	Aperture	Focal Length	Sensor Size
Xiaomi Mi A1	12MP	f/2.2	26mm	1.25um
Samsung S8	12MP	f/1.7	26mm	1.4um
Samsung S21	12MP	f/1.8	26mm	1.8um

TABLE III
VALUES OF WATERMARK IMPERCEPTIBILITY METRICS

α	Document images		Common images	
	<i>PSNR</i> , dB	<i>SSIM</i>	<i>PSNR</i> , dB	<i>SSIM</i>
3/255	44.4	0.9992	47.5	0.9972
4/255	42.6	0.9991	45.5	0.9958
5/255	40.6	0.9989	43.8	0.9942
6/255	39.0	0.9987	42.4	0.9926
7/255	37.7	0.9985	41.1	0.9910
8/255	36.5	0.9983	40.0	0.9894
9/255	35.4	0.9980	39.0	0.9878
10/255	34.5	0.9977	38.1	0.9863

To determine the minimal appropriate opacity value α , we checked the accuracy of the watermark extraction. Shooting was performed with 9 pairs of cameras and monitors in a given range of α values at the distance of 40 centimeters between camera and monitor. For each pair and each opacity value, 10 photographs of documents of various sizes displayed on the monitor screen were taken. Watermarks were extracted from the photographs and compared to the embedded watermarks. We calculated Bit Error Rate (BER) — the average amount of inverted bits in extracted watermark before error correction. If the value of BER is close to 0, almost all watermarks were extracted correctly. As we use error correction codes, we also counted number of photographs with no more than 3 errors in the extracted watermark. After error correction, these watermarks correspond to the embedded watermarks. The results of the experiment are presented in the Table IV.

At $\alpha \geq 7/255$, the watermark is correctly extracted from

TABLE IV
ACCURACY OF WATERMARK EXTRACTION FOR VARIOUS OPACITY VALUES

α	Camera					
	Xiaomi Mi A1	Samsung S8	Samsung S21	Samsung SyncMaster 940FN Monitor	Sony SDM-S75A Monitor	
BER ≤ 3 err.	BER ≤ 3 err.	BER ≤ 3 err.	BER ≤ 3 err.	BER ≤ 3 err.	BER ≤ 3 err.	
3/255	33.6%	3/10	18.4%	7/10	17.6%	6/10
4/255	9.1%	7/10	1.4%	10/10	6.8%	9/10
5/255	10.6%	7/10	0.6%	10/10	0.2%	10/10
6/255	1.0%	10/10	0.4%	10/10	0.2%	10/10
7/255	0.6%	10/10	0.0%	10/10	0.2%	10/10
8/255	0.2%	10/10	0.0%	10/10	0.2%	10/10
9/255	0.2%	10/10	0.0%	10/10	0.0%	10/10
10/255	0.0%	10/10	0.0%	10/10	0.0%	10/10
Dell U2722D Monitor						
3/255	7.8%	8/10	8.8%	8/10	14.8%	7/10
4/255	1.8%	9/10	1.4%	10/10	1.2%	10/10
5/255	1.0%	10/10	1.0%	10/10	1.0%	10/10
6/255	0.8%	10/10	0.6%	10/10	0.4%	10/10
7/255	0.2%	10/10	0.2%	10/10	0.0%	10/10
8/255	0.0%	10/10	0.2%	10/10	0.0%	10/10
9/255	0.0%	10/10	0.0%	10/10	0.0%	10/10
10/255	0.0%	10/10	0.2%	10/10	0.0%	10/10

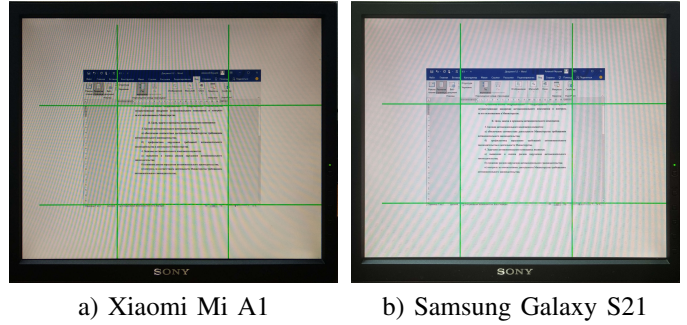


Fig. 7. Photographs of the Sony SDM-S75A monitor at the distance of 40 cm. Green lines on document borders are used for automatic perspective correction and photograph cropping, both can be done manually in practical application.

almost all photographs, except for photographs of the Sony SDM-S75A monitor screen taken with the cameras of Xiaomi Mi A1 and Samsung Galaxy S21 smartphones. These photographs are strongly distorted with the moiré effect (Fig. 7). In the following experiments, α values were fixed for each monitor: 7/255 for the Samsung SyncMaster 940FN monitor, 8/255 for the Sony SDM-S75A monitor, 6/255 for the Dell U2722D monitor.

B. The Impact of Shooting Distance on the Extraction Accuracy

For all pairs of monitors and cameras, photographs were taken at different distances between the camera and the screen. The results of watermark extraction are shown in the Table V.

As in the previous experiment, there is a high error percentage in watermarks extracted from photographs of the Sony SDM-S75A monitor screen taken with the cameras of Xiaomi Mi A1 and Samsung Galaxy S21 smartphones at the distance of 40 cm. Meanwhile, the extraction accuracy at other

TABLE V
THE IMPACT OF SHOOTING DISTANCE ON THE WATERMARK EXTRACTION ACCURACY

Distance	Camera			
	Xiaomi Mi A1	Samsung S8	Samsung S21	
BER ≤ 3 err.	BER ≤ 3 err.	BER ≤ 3 err.	Samsung SyncMaster 940FN Monitor	
25 cm	1.6%	10/10	45.0%	0/10
40 cm	0.4%	10/10	0.2%	10/10
60 cm	0.0%	10/10	0.8%	10/10
80 cm	0.6%	10/10	1.2%	10/10
100 cm	0.4%	10/10	1.2%	9/10
Sony SDM-S75A Monitor				
25 cm	34.0%	3/10	4.8%	8/10
40 cm	32.0%	4/10	0.8%	10/10
60 cm	0.6%	10/10	0.6%	10/10
80 cm	0.4%	10/10	1.2%	10/10
100 cm	0.8%	10/10	2.0%	10/10
Dell U2722D Monitor				
25 cm	27.8%	4/10	9.6%	5/10
40 cm	1.0%	10/10	1.2%	10/10
60 cm	0.4%	10/10	7.0%	9/10
80 cm	0.2%	10/10	4.4%	9/10
100 cm	0.2%	10/10	4.4%	9/10

distances is much higher. This happens due to the fact that increased moiré effect in photography occurs under certain shooting conditions, including the distance between the camera and the screen. Also, on other pairs of monitors and cameras, the moiré effect appears at the distance of 25 cm.

C. The Impact of Shooting Angle on the Extraction Accuracy

To test the effect of photographic perspective distortion on the accuracy of watermark extraction, photographs were taken at different horizontal angles. The distance between the camera and the center of the screen was fixed at 40 cm. The results of the experiment are listed in the Table VI.

Watermark extraction from photographs of the Sony SDM-S75A monitor taken with the cameras of Xiaomi Mi A1 and Samsung Galaxy S21 smartphones shows controversial result. Photographs with a large perspective distortion are less prone to the moiré effect (Fig. 8), which results in a higher watermark extraction accuracy. The moiré effect also appears in the photographs of the Samsung SyncMaster 940FN monitor, taken with the camera of the Xiaomi Mi A1 smartphone at the angle of 15°, decreasing watermark extraction accuracy.

D. The Impact of JPEG Compression Quality on the Extraction Accuracy

The proposed document watermarking method was tested for robustness to JPEG image compression. 50 photographs

TABLE VII
THE IMPACT OF JPEG COMPRESSION QUALITY ON THE WATERMARK EXTRACTION ACCURACY

JPEG quality	Average file size, KB	BER	≤ 3 errors
Uncompressed	4589	1.3%	50/50
80	1870	1.2%	50/50
60	1211	1.2%	50/50
50	1048	1.4%	49/50
40	900	1.4%	49/50
30	748	4.4%	46/50
20	573	8.5%	42/50
15	478	14.5%	34/50
10	376	26.9%	20/50

with less than 3 extraction errors from previous experiments were selected randomly. The photographs were compressed using the JPEG algorithm with different values of quality. Compressed images extraction accuracy is presented in the Table VII.

The watermark is completely extracted from photographs after compression by the JPEG algorithm with at least 40 JPEG quality, and is also partially extracted with the quality at least 20.

V. CONCLUSION

Based on the existing approaches study and problem analysis, a new method for marking images of text documents displayed on a monitor screen has been developed. A program for embedding a digital watermark on the monitor screen and a program for extracting a digital watermark from a screen photograph have been implemented. The overlay image with the watermark is static and depends only on the encoded message and not on the screen image. Due to the static nature of the method, the watermark embedding program consumes low computational resources. Imperceptibility metrics have been calculated, according to which the watermark is considered invisible to the device user. The proposed watermarking method was tested for the accuracy of extracting encoded message from a photograph for different pairs of camera and monitor, different distances from the camera to the screen, different angles between the camera and the screen. Testing has shown high accuracy in extracting a message from screen photographs, with the exception of photographs taken in certain conditions. The robustness of the watermarking method to the JPEG compression algorithm has been checked. The main directions for further work are to increase of imperceptibility of the watermark on the screen and to improve the accuracy of watermark extraction from screen photographs. The method shows low extraction accuracy from screen photographs with a strong moiré effect. To solve this problem, it is necessary to study the possibility of applying existing methods for removing the moiré effect from screen photographs.

TABLE VI
THE IMPACT OF PERSPECTIVE ANGLE ON THE WATERMARK EXTRACTION ACCURACY

Angle	Camera					
	Xiaomi Mi A1		Samsung S8		Samsung S21	
	BER	≤ 3 err.	BER	≤ 3 err.	BER	≤ 3 err.
Samsung SyncMaster 940FN Monitor						
0°	0.4%	10/10	0.2%	10/10	0.8%	10/10
15°	0.8%	10/10	0.4%	10/10	1.2%	10/10
30°	14.6%	6/10	1.0%	10/10	1.6%	9/10
45°	0.4%	9/10	1.2%	10/10	0.2%	10/10
60°	1.2%	10/10	1.4%	10/10	1.8%	10/10
Sony SDM-S75A Monitor						
0°	32.0%	4/10	0.8%	10/10	22.0%	6/10
15°	8.4%	8/10	1.6%	10/10	15.0%	7/10
30°	2.0%	10/10	1.8%	10/10	1.4%	10/10
45°	2.4%	10/10	1.4%	10/10	1.4%	10/10
60°	1.4%	10/10	1.6%	10/10	1.0%	8/10
Dell U2722D Monitor						
0°	1.0%	10/10	1.2%	10/10	0.8%	10/10
15°	6.6%	8/10	7.4%	9/10	1.4%	10/10
30°	1.4%	10/10	7.4%	9/10	1.8%	10/10
45°	1.8%	10/10	3.8%	9/10	1.4%	10/10
60°	1.6%	9/10	6.8%	9/10	1.2%	10/10

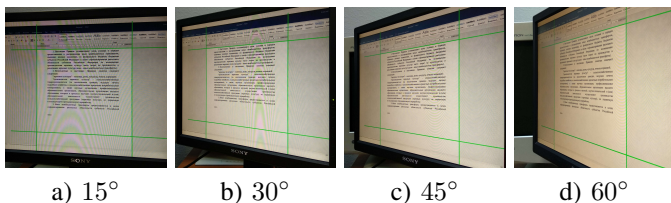


Fig. 8. Photographs of the Sony SDM-S75A monitor at the distance of 40 cm with different perspective angles.

REFERENCES

[1] “Russia: restricted information leaks, 2020,” InfoWatch Analytics Center, 2021.

[2] J. T. Brassil, S. Low, N. F. Maxemchuk, and L. O’Gorman, “Electronic marking and identification techniques to discourage document copying,” *IEEE Journal on Selected Areas in Communications*, vol. 13, no. 8, pp. 1495–1504, 1995.

[3] I. J. Cox, J. Kilian, F. T. Leighton, and T. Shamoon, “Secure spread spectrum watermarking for multimedia,” *IEEE transactions on image processing*, vol. 6, no. 12, pp. 1673–1687, 1997.

[4] F. Hartung and M. Kutter, “Multimedia watermarking techniques,” *Proceedings of the IEEE*, vol. 87, no. 7, pp. 1079–1107, 1999.

[5] A. Pramila, A. Keskinarkaus, and T. Seppänen, “Multiple domain watermarking for print-scan and jpeg resilient data hiding,” in *Digital Watermarking*, 2008, pp. 279–293.

[6] P. Dong and N. Galatsanos, “Affine transformation resistant watermarking based on image normalization,” vol. 3, 2002, pp. 489–492.

[7] M. Taleby Ahvanooy, Q. Li, H. J. Shim, and Y. Huang, “A comparative analysis of information hiding techniques for copyright protection of text documents,” *Security and Communication Networks*, vol. 2018, pp. 1–22, 2018.

[8] D. Gugelmann, D. Sommer, V. Lenders, M. Happe, and L. Vanbever, “Screen watermarking for data theft investigation and attribution,” in *2018 10th International Conference on Cyber Conflict (CyCon)*. IEEE, 2018, pp. 391–408.

[9] A. Y. Yakushev, Y. V. Markin, S. A. Fomin, D. O. Obydenkov, and B. V. kondrat’ev, “Text documents screen watermarking by changing background brightness in the interline spacing,” *Proceedings of the Institute for System Programming of the RAS (Proceedings of ISP RAS)*, vol. 33, no. 4, pp. 147–162, 2021.

[10] D. O. Obydenkov, A. Y. Yakushev, Y. V. Markin, A. E. Frolov, S. A. Fomin, S. V. Kozlov, D. D. Gromey, A. V. Kozachok, and B. V. Kondrat’ev, “Document marking system for leak investigations,” *Proceedings of the Institute for System Programming of the RAS (Proceedings of ISP RAS)*, vol. 33, no. 6, pp. 161–174, 2021.

[11] S. Ge, J. Fei, Z. Xia, Y. Tong, J. Weng, and J. Liu, “A screen-shooting resilient document image watermarking scheme using deep neural network,” *IET Image Processing*, 2022.

[12] H. Fang, W. Zhang, Z. Ma, H. Zhou, S. Sun, H. Cui, and N. Yu, “A camera shooting resilient watermarking scheme for underpainting documents,” *IEEE Transactions on Circuits and Systems for Video Technology*, vol. 30, no. 11, pp. 4075–4089, 2019.

[13] H. Fang, D. Chen, F. Wang, Z. Ma, H. Liu, W. Zhou, W. Zhang, and N. Yu, “TERA: Screen-to-camera image code with transparency, efficiency, robustness and adaptability,” *IEEE Transactions on Multimedia*, vol. 24, pp. 955–967, 2021.

[14] Y. Cheng, X. Ji, L. Wang, Q. Pang, Y.-C. Chen, and W. Xu, “mID: Tracing screen photos via Moiré patterns,” in *30th USENIX Security Symposium (USENIX Security 21)*, 2021, pp. 2969–2986.

[15] S. Yuan, R. Timofte, A. Leonardis, and G. Slabaugh, “Ntire 2020 challenge on image demoireing: Methods and results,” in *Proceedings of the IEEE/CVF Conference on Computer Vision and Pattern Recognition Workshops*, 2020, pp. 460–461.

[16] Y. Sun, Y. Yu, and W. Wang, “Moiré photo restoration using multiresolution convolutional neural networks,” *IEEE Transactions on Image Processing*, vol. 27, no. 8, pp. 4160–4172, 2018.

[17] O. Ronneberger, P. Fischer, and T. Brox, “U-net: Convolutional networks for biomedical image segmentation,” in *International Conference on Medical image computing and computer-assisted intervention*. Springer, 2015, pp. 234–241.

[18] T.-H. Wang, H.-J. Huang, J.-T. Lin, C.-W. Hu, K.-H. Zeng, and M. Sun, “Omnidirectional CNN for visual place recognition and navigation,” in *2018 IEEE International Conference on Robotics and Automation (ICRA)*. IEEE, 2018, pp. 2341–2348.

[19] M. Tan and Q. Le, “EfficientNet: rethinking model scaling for convolutional neural networks,” in *International conference on machine learning*. PMLR, 2019, pp. 6105–6114.

[20] O. Russakovsky, J. Deng, H. Su, J. Krause, S. Satheesh, S. Ma, Z. Huang, A. Karpathy, A. Khosla, M. Bernstein *et al.*, “ImageNet large scale visual recognition challenge,” *International journal of computer vision*, vol. 115, no. 3, pp. 211–252, 2015.

[21] T. Porter and T. Duff, “Compositing digital images,” in *Proceedings of the 11th annual conference on Computer graphics and interactive techniques*, 1984, pp. 253–259.

[22] D. P. Kingma and J. Ba, “Adam: A method for stochastic optimization,” *arXiv preprint arXiv:1412.6980*, 2014.

[23] R. C. Bose and D. K. Ray-Chaudhuri, “On a class of error correcting binary group codes,” *Information and control*, vol. 3, no. 1, pp. 68–79, 1960.

[24] “List of documents on the website of the Ministry of Science and Higher Education of the Russian Federation.” [Online]. Available: <https://minobrnauki.gov.ru/documents/>

[25] “List of documents on the website of the Ministry of Finance of the Russian Federation.” [Online]. Available: <https://archive.minfin.gov.ru/en/>

[26] Z. Wang, A. C. Bovik, H. R. Sheikh, and E. P. Simoncelli, “Image quality assessment: from error measurement to structural similarity,” *IEEE transactions on image processing*, vol. 13, no. 1, 2004.

[27] A. Kuznetsova, H. Rom, N. Alldrin, J. Uijlings, I. Krasin, J. Pont-Tuset, S. Kamali, S. Popov, M. Malluci, A. Kolesnikov *et al.*, “The open images dataset v4,” *International Journal of Computer Vision*, vol. 128, no. 7, pp. 1956–1981, 2020.